

# Determination of $\alpha$ -Tocopherol in Vegetable Oils Using a Molecularly Imprinted Polymers–Surface-Enhanced Raman Spectroscopic Biosensor

Shaolong Feng,<sup>†,§</sup> Fang Gao,<sup>§,#</sup> Zhiwen Chen,<sup>#</sup> Edward Grant,<sup>#</sup> David D. Kitts,<sup>§</sup> Shuo Wang,<sup>\*,†</sup> and Xiaonan Lu<sup>\*,§</sup>

<sup>†</sup>Key Laboratory of Food Nutrition and Safety, Ministry of Education of China, Tianjin University of Science and Technology, Tianjin 300457, China

<sup>§</sup>Food, Nutrition and Health Program, Faculty of Land and Food Systems, The University of British Columbia, Vancouver, British Columbia V6T 1Z4, Canada

<sup>#</sup>Department of Chemistry, The University of British Columbia, Vancouver, British Columbia V6T 1Z1, Canada

## **S** Supporting Information

**ABSTRACT:** We report the development of a novel hybrid “capture–detection” molecularly imprinted polymers–surface-enhanced Raman spectroscopic (MIPs-SERS) biosensor for the detection and quantification of  $\alpha$ -tocopherol ( $\alpha$ -Toc) in vegetable oils.  $\alpha$ -Toc served as the template for MIPs synthesis. Methacrylic acid formed as the functional monomer. Ethylene glycol dimethacrylate was the cross-linking agent, and 2,2'-azobisisobutyronitrile was used as the initiator. The synthesized MIPs functioned to rapidly and selectively adsorb and separate  $\alpha$ -Toc from oil components. We validated a dendritic silver nanostructure synthesized by a displacement reaction to be a suitable SERS substrate for the enhancement of Raman signals. Second-derivative transformations and chemometric models based upon SERS spectral features confirmed the possibility of a rapid and precise detection and quantification of different spiking levels of  $\alpha$ -Toc in four different sources of vegetable oils (Mahalanobis distance from 15.93 to 34.01 for PCA model;  $R > 0.92$ , RMSE  $< 0.41$  for PLSR model). The MIPs-SERS biosensor had a high sensitivity as well as a good recovery for  $\alpha$ -Toc analysis in vegetable oils. The entire analysis required 15 min or less to complete with limited sample preparation.

**KEYWORDS:** MIPs, SERS, vitamin, biosensing system

## ■ INTRODUCTION

Tocopherol is an important fat-soluble vitamin that possesses significant antioxidant activity. It contributes to maintaining the integrity of intracellular membranes by protecting physical and physiological stability and providing a well-defined defense against oxidative tissue damage.<sup>1</sup> Humans obtain tocopherol mainly from vegetable oils, milk, fruits, and vegetables.<sup>2</sup> Tocopherol is composed of four isoforms in many vegetable oils with  $\alpha$ -tocopherol ( $\alpha$ -Toc) being the principal isoform in some oils as well as the most relevant one in human circulation.<sup>3</sup> To meet labeling requirements and to ensure that appropriate levels are maintained following processing of vegetable oil and milk products, the food and dietary supplement industries require a means for the rapid and precise determination of  $\alpha$ -Toc. Measured  $\alpha$ -Toc level is a significant indicator of quality of food lipids and related formulations.<sup>4</sup> For example, with some food processing and storage conditions,  $\alpha$ -Toc will react with peroxy radicals, ultimately forming tocopheroxide, tocopheryl hydroquinone, and tocopheryl quinone. These degradation products of  $\alpha$ -Toc exhibit little or no vitamin activity.<sup>2</sup> Furthermore,  $\alpha$ -Toc is viewed as the sole form exhibiting vitamin E activity.<sup>5</sup> The current method for determination of  $\alpha$ -Toc in foods involves liquid chromatography,<sup>6</sup> which is laborious, and time-consuming and requires solvents for extraction. Other methods

include spectrophotometric and direct fluorometric procedures, which are rapid but less accurate. Therefore, alternative detection methods are needed.

Surface-enhanced Raman spectroscopy (SERS) has progressed rapidly during the past decade as a fast and reliable detection tool for the determination of trace levels of chemical compounds and microbiological agents<sup>7,8</sup> in foods and biological tissues. The induction of an electromagnetic field when the analyte molecules are in proximity to the surface of the roughened gold and/or silver nanostructures generates a localized surface plasmon resonance, resulting in significant enhancement of faint Raman scattering signals derived from low concentrations of analyte molecules.<sup>9</sup> Some studies reported enhancement factors as great as  $10^{15}$  for active Raman reporting molecules (e.g., pyridine), resulting in detection limits approaching the single-molecule level.<sup>10</sup> SERS substrates can be fabricated either by “bottom-up” (e.g., self-assembly of chemicals) or “top-down” technique (e.g., electrobeam lithography).<sup>10</sup>

**Received:** September 3, 2013

**Revised:** October 2, 2013

**Accepted:** October 7, 2013

**Published:** October 7, 2013

The use of SERS for the detection of specific analytes in complicated matrices (e.g., foods) suffers the complication that other components besides the analyte can also contribute spectral features to the SERS signal, causing difficulties in spectral interpretation and chemometric model construction. This has motivated sample pretreatment, such as extraction by organic solvents and centrifugation to remove interferences from food matrices, combined with the multivariate analysis of second-derivative transformed spectra to differentiate features of analyte molecules from ones owing to remaining interference residues. Even though some research has validated the success of such methods for the detection of specific chemical hazards (e.g., antibiotic residues, veterinary drugs, melamine, Sudan red) in food matrices, it does require the analyte molecules to have at least one unique functional group with a specific vibrational mode to generate a featured band at a definite wavenumber.<sup>11–14</sup> For example, the SERS spectral band at  $\sim 680\text{ cm}^{-1}$ , assigned to a unique ring breathing mode involving the in-plane deformation of the triazine ring in melamine, can be applied to the identification of melamine in various food systems, such as chicken feeds, cakes, and noodles.<sup>13</sup>

Recent methods to overcome the matrix interference seek to capture, separate, and enrich specific analyte molecules first and then apply SERS for the reliable detection. For instance, researchers have applied antibody-based methods to separate specific allergenic and toxic proteins from milk followed by SERS determination.<sup>15</sup> In addition, aptamer-based SERS has been established to separate and detect food chemical hazards and pathogens, such as ricin,<sup>16</sup> *Staphylococcal* enterotoxin B,<sup>17</sup> and bacterial spores.<sup>18</sup> However, the synthesis and manufacture of aptamer for recognition and capture of specific analytes is time-consuming and expensive, and all of the current aptamer–SERS publications have used commercially available aptamers for conjugation with SERS substrates, which significantly limits the categories of analytes that can be determined.

Molecularly imprinted polymers (MIPs) offer a new technique for efficient separation and enrichment of specific analyte molecules from complicated matrices including foods.<sup>19</sup> In molecular imprinting, the target molecule acts as the template and can interact with functional monomers and cross-linking agents by copolymerization to form a shell.<sup>20</sup> Due to superior stability and specificity, MIPs show promise as recognition elements in various categories of sensors. Numerous studies have validated the potential of MIPs for specific recognition and binding to analyte molecules in complicated matrices.<sup>20</sup> MIPs have also been coupled with high-performance liquid chromatography (HPLC), quantum dots, and graphene oxide for the detection of chemical compounds. For instance, molecularly imprinted solid phase extraction (SPE) has been developed for the selective HPLC determination of  $\alpha$ -Toc in bay leaves.<sup>21</sup> Recently, a novel molecular polymer imprinted on ionic liquid-modified quantum dots with/without graphene oxide has shown promise as an optosensing system for specific recognition of vitamin E.<sup>22,23</sup> So far, no one has reported a MIPs-SERS biosensing system for the detection of specific analyte molecules from complicated food matrices. The present study describes the first application of a MIPs-SERS biosensing system for the detection of  $\alpha$ -Toc from four different types of vegetable oils.

## MATERIALS AND METHODS

**Chemicals and Reagents.** Methacrylic acid (MAA), ethylene glycol dimethacrylate (EGDMA), 2,2'-azobis(isobutyronitrile)

(AIBN),  $\alpha$ -Toc, 6-hydroxy-2,5,7,8-tetramethylchroman-2-carboxylic acid (Trolox), 2,5-di-*tert*-butylhydroquinone (DBHQ), silver nitrite, zinc plate (99.99% purity), chloroform, ethanol, methanol, acetic acid, hexane, and hydrochloric acid were purchased from Sigma-Aldrich (St. Louis, MO, USA). All of the chemical agents are of at least reagent grade. The samples of peanut oil, corn oil, olive oil, and canola oil were obtained from local retail sources.

**Synthesis of MIPs.** MAA and EGDMA were purified by reduced-pressure distillation before use. The synthesis of the MIPs was then conducted according to the following procedures: 1 mmol of  $\alpha$ -Toc was dissolved in 5.25 mL of chloroform and then mixed with 8 mmol of MAA. The mixture was stirred for 30 min at 22 °C before the addition of 25 mmol of cross-linking agent EGDMA and 0.045 g of initiator AIBN. The solution was purged with nitrogen for 15 min. The mixture was sealed, and thermal polymerization was initiated in an oil bath at 60 °C for 24 h. After the polymerization, the rigid polymer was crushed and sieved through a 200 mesh steel sieve, and the template was subsequently removed by Soxhlet extraction with 200 mL of methanol/acetic acid (9:1, v/v) for 24 h, followed by extraction with 200 mL of methanol for another 24 h until no  $\alpha$ -Toc was detected using UV spectrometry (292 nm). After Soxhlet extraction, the synthesized MIPs product was dried overnight in a vacuum drying oven at 60 °C. For comparison, nonimprinted polymers (NIPs) were also prepared following the same procedure in the absence of template (i.e.,  $\alpha$ -Toc).

**Adsorption Test.** The static and kinetic adsorption tests were conducted individually. To measure the capacity for static adsorption, 50 mg of MIPs or NIPs was mixed with 10 mL of ethanol solution (ethanol/water, 6:4, v/v) of  $\alpha$ -Toc at different concentrations (i.e., 10, 20, 30, 40, 60, 80, and 100 mg/L). The mixture was shaken at 200 rpm at 22 °C for 120 min and then centrifuged at 4000g at 22 °C for 15 min. The supernatant was measured for the unbound  $\alpha$ -Toc by UV spectrometry at 292 nm. The adsorption capacity of MIPs toward the analogue of  $\alpha$ -Toc, namely, Trolox and DBHQ (Supporting Information Figure S1), was also measured to determine  $\alpha$ -Toc selectivity of the MIPs. This procedure was also applied to test the static adsorption capacity of NIPs. The adsorption capacity was calculated using the method of Qian et al.<sup>24</sup>

For kinetic tests, 50 mg of MIPs was mixed with  $\alpha$ -Toc (100 mg/L) in 10 mL of ethanol solution. The mixture was shaken (200 times/min) for various time intervals (i.e., 5, 10, 15, 20, 30, 40, 60, 90, 120, and 180 min) at 22 °C and then centrifuged at 4000g for 15 min. The unbound  $\alpha$ -Toc in the supernatant was measured by UV spectrometry at 292 nm.

**Pretreatment of Vegetable Oils.** This study used four different types of vegetable oils, namely, peanut oil, olive oil, corn oil, and canola oil. Tocopherols were recovered following the protocols of Gimeno et al.<sup>25</sup> Briefly, mixtures of vegetable oil in hexane (200  $\mu$ L; 10% w/v), ethanol (200  $\mu$ L), and methanol (600  $\mu$ L) were vortex-mixed for 30 s and then separated by centrifugation at 4000g for 5 min at 4 °C. The top layer (500  $\mu$ L) was collected and passed through a 0.22  $\mu$ m nylon filter before HPLC determination.

**High-Performance Liquid Chromatography.** The chromatographic conditions for  $\alpha$ -Toc quantitation were patterned after the study by Bonvehi et al.,<sup>26</sup> with modification. Briefly, HPLC analyses were conducted using an Agilent 1100 series HPLC with a photodiode array detector (DAD) set at a wavelength of 292 nm.  $\alpha$ -Toc was separated by injecting a 40  $\mu$ L sample onto a Waters  $\mu$ Bondapak-C<sub>18</sub> (3.9  $\times$  300 mm diameter) column coupled to a Waters  $\mu$ Bondapak-C<sub>18</sub> guard column at 35 °C. At least three separate injections were conducted for each sample extract. HPLC grade solvents of 95% CH<sub>3</sub>OH and 5% H<sub>2</sub>O were used as mobile phase at a flow rate of 2 mL/min over a total run time of 8 min.

**Molecularly Imprinted Solid Phase Extraction.** Dried MIPs or NIP particles (500 mg) were packed into a 6 mL polypropylene SPE column with two PTFE frits (Agilent, Santa Clara, CA, USA) at each end. The molecularly imprinted SPE cartridge was conditioned first with 2 mL of acetonitrile and then with 2 mL of ethanol. After that, it was equilibrated with 2 mL of hexane and then with the loading solvent (sample containing  $\alpha$ -Toc).

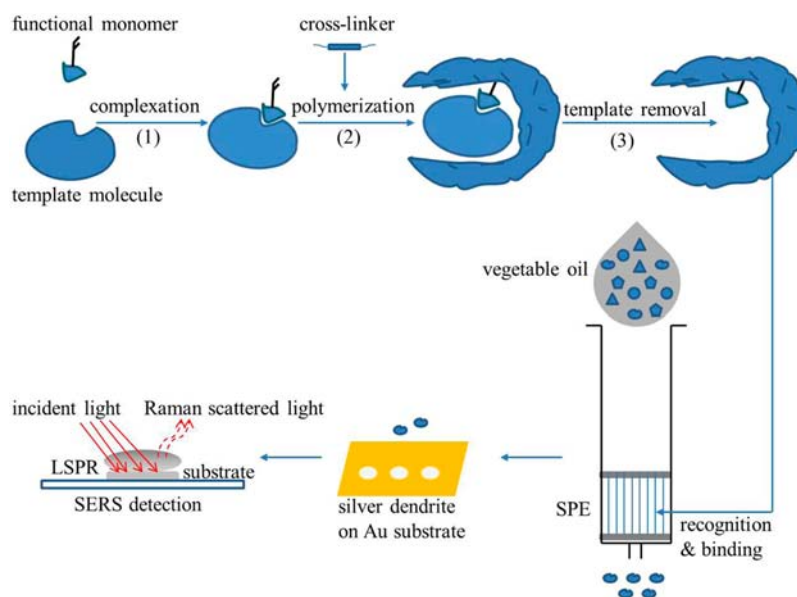


**Figure 1.** Schematic illustration of the molecularly imprinted polymers–surface-enhanced Raman spectroscopic (MIPs-SERS) biosensing system for detection of  $\alpha$ -tocopherol in vegetable oils. SPE, solid phase extraction; LSPR, localized surface plasmon resonance.

Vegetable oils from different sources (0.05 g) were spiked with different amounts of  $\alpha$ -Toc (i.e., 0, 0.1, 0.5, 1 mg) and then dissolved in 5 mL of hexane. After 30 s of vortex mixing, 2 mL of each sample solution was loaded through the molecularly imprinted SPE column with a flow rate of 1.5 mL/min. Then, 3 mL of washing solvent (hexane) was passed through the cartridges with a flow rate of 1.5 mL/min, followed by another wash using 60% ethanol (3 mL) with a flow rate of 1.5 mL/min. After the column had dried, 5 mL of ethanol with 5% acetic acid was used to elute  $\alpha$ -Toc, and the flow rate was 1 mL/min. The eluted solution (2  $\mu$ L) was dried under nitrogen and redissolved in 2  $\mu$ L of ethanol solution (60%, v/v). This solution was directly deposited onto the SERS-active nanosubstrate for spectral collection.

**Synthesis of Silver Dendrite Nanostructure.** Recent reports described the synthesis and growth of silver dendrite nanostructure by displacement on different commercial foils (e.g., zinc, aluminum, copper).<sup>27–29</sup> Presently, silver dendrite nanostructures were synthesized following the method of Fang et al.<sup>29</sup> with minor modifications. The zinc foil (99.99% purity) was first treated and cleaned using hydrochloric acid (0.02 mol/L) to remove the surface contamination and oxidative byproducts (e.g., ZnO) and then rinsed with distilled water. The cleaned zinc foil was immersed into 200 mM AgNO<sub>3</sub> solution and allowed to react at 22 °C. We attained silver nanostructures with different morphologies by adjusting the silver ion concentration after different reaction times. The silver dendrite products were then peeled off the zinc foil and washed with distilled water in an ultrasonic bath and then transferred to glass vials. These products can be used as SERS-active substrates for storage up to 6 months. For use in a SERS experiment, the silver dendrite nanostructure was deposited onto a gold-coated microarray chip (Thermo Electron, Waltham, MA, USA) to generate multiple spots.<sup>30</sup> After drying under cold nitrogen flow, the silver dendrite spots were ready to be used for SERS spectral collection. The nanostructure of silver dendrite was examined using scanning electron microscopy (Hitachi SU1500, Tokyo, Japan), and the scan was conducted at high-vacuum mode at the electron acceleration voltage of 10 kV.

**Raman Spectroscopic Instrumentation.** This study used a confocal micro-Raman spectroscopic system coupled with a 785 nm near-infrared laser. This system includes a Raman spectrometer (Renishaw, Gloucestershire, UK) and a Leica microscope (Leica Biosystems, Wetzlar, Germany). The spectrometer has an entrance aperture of 50  $\mu$ m and a focal length of 300 mm and is equipped with a 1200 line/mm grating. Interference filters completely eliminate Rayleigh scattered light, leaving a pure Raman signal to be dispersed

by the spectrometer and recorded by a 578 by 385 pixel charge-coupled device (CCD) array detector, with a pixel size of 22  $\mu$ m.

A gold-coated microarray chip covered with multiple silver dendrite spots was mounted onto a standard stage of the microscope, focused under the collection assembly, and the SERS spectra were recorded by using a 50 $\times$  Nikon objective (NA = 0.75, WD = 0.37 mm) over a wavenumber range of 400–1800  $\text{cm}^{-1}$ . We collected spectra for each sample using a 10 s exposure at eight random locations on each spot with an incident laser power for illumination of  $\sim$ 0.1 mW. The system operated under the control of WiRE 3.4 software (Renishaw). All experiments were carried out at least in triplicate.

**Spectral Analysis and Chemometric Models.** Collected SERS spectra were first processed by binning (2  $\text{cm}^{-1}$ ) and then smoothing (9-point Savitzky-Golay algorithm) to reduce spectral noise,<sup>31</sup> followed by normalization of all the spectra with reference to the band at 1072  $\text{cm}^{-1}$ , corresponding to the signal from NO<sub>3</sub><sup>−</sup> from the SERS substrate, which served as an internal standard.<sup>30</sup>

We applied second-derivative transformation to the preprocessed SERS spectra. The second-derivative transformed SERS spectrum can swing with greater amplitude than the original spectrum to magnify minor spectral variation and separate overlapping bands.<sup>32</sup> This transformation is a good noise filter in that the variations of the Raman spectral baseline have insignificant impact on second derivatives.<sup>31</sup>

Unsupervised principal component analysis (PCA) served to reveal variations between samples/treatments without a priori knowledge. We took the Mahalanobis distance provided by the PCA model as a measure of the distance between the centroids of different classes.<sup>9</sup> The partial least-squares regression (PLSR) model was then constructed to predict sample concentration for sets of vegetable oil samples spiked with  $\alpha$ -Toc according to the method of standard additions. PLSR models were tested using leave-one-out cross-validation.<sup>33</sup>

## RESULTS AND DISCUSSION

Figure 1 provides a detailed schematic illustration of this MIPs-SERS biosensing system for the determination of  $\alpha$ -Toc isoform in different vegetable oils. This biosensing system employs the two steps of separation by MIPs and detection by SERS. With the availability of the synthesized MIPs and SERS nanosubstrate, detection and quantification of  $\alpha$ -Toc in vegetable oils required a total analysis time of <15 min. The procedure consisted of treating the vegetable oil sample with

hexane for 30 s followed by three steps of MIPs-SPE, namely, loading (1.5 min), washing (4 min), and eluting (5 min). After 1 min of drying, Raman spectral collection was conducted (10 s).

The concentrations of  $\alpha$ -Toc from the four different sources of vegetable oils determined using HPLC-DAD were relatively similar with values ranging around 0.2 mg/g. This result conforms with previous reports.<sup>26</sup> HPLC confirmed the adsorption effect of MIPs in the spiking experiment. Figure S1 (Supporting Information) shows a representative chromatograph of canola oil spiked with  $\alpha$ -Toc after MIPs adsorption.

**MIPs for Separation and Enrichment of  $\alpha$ -Toc in Vegetable Oils.** The present study employed a noncovalent bulk polymerization method for the synthesis of MIPs to specifically recognize, separate, and enrich  $\alpha$ -Toc present in vegetable oils. This method has been similarly applied for the determination of various chemical compounds in foods, such as metolcarb in fruits and vegetables,<sup>24</sup> ractopamine<sup>34</sup> and methimazole<sup>35</sup> in pork samples, and quinoxaline-2-carboxylic acid and methyl-3-quinoxaline-2-carboxylic acid in animal muscles in general.<sup>36</sup>

We determined the adsorption capacity of the synthesized MIPs to evaluate the recognition and binding capacity of the template. Figure 2A shows the adsorption isotherm curve. The adsorption capacity of MIPs or NIPs improved with the increase of the initial concentration of  $\alpha$ -Toc. Specifically, the adsorption capacity of MIPs ( $\sim 2.49$  mg/g) was approximately 2 times that of NIPs ( $\sim 1.30$  mg/g) for  $\alpha$ -Toc at the concentration of 100 mg/L. Therefore, MIPs had a higher adsorption capacity for  $\alpha$ -Toc than NIPs. Generally, increasing

the polarity of the solution reduces the adsorption capacity in both cases.

Scatchard relationship was determined to assess the affinity of MIPs and NIPs toward  $\alpha$ -Toc (Figure 2B). Here, we constructed a Scatchard plot using the expression  $Q/C = -Q/K_d + Q_{\max}/K_d$ , where  $Q$  is the adsorption capacity at adsorption equilibrium,  $C$  is the initial concentration of analyte (i.e.,  $\alpha$ -Toc),  $K_d$  is the distribution coefficient, and  $Q_{\max}$  is the saturated adsorption capacity.<sup>24</sup> The adsorption isotherm of MIPs for  $\alpha$ -Toc showed a good linear regression ( $R^2 = 0.97$ ). The  $Q_{\max}$  of MIPs for  $\alpha$ -Toc was 4.53 mg/g. By contrast, NIPs showed nonlinearity, indicating no selective adsorption sites for  $\alpha$ -Toc. We infer from this that the absorption by MIPs is mainly driven by hydrogen binding, whereas the interaction between NIPs and  $\alpha$ -Toc arises from nonspecific adsorption.

We conducted kinetic adsorption tests to evaluate the adsorption rate of MIPs. The equilibration of 50 mg of MIPs with 10 mL of  $\alpha$ -Toc (100 mg/L) for multiple time intervals at 22 °C confirmed that the synthesized MIPs effectively adsorbed  $\alpha$ -Toc and reached a binding equilibrium within 30 min. This proves the feasibility for rapid separation and enrichment of  $\alpha$ -Toc in different vegetable oils. It is worth noting that saturation time was shorter when the concentration of  $\alpha$ -Toc was lower.

The selectivity of MIPs toward  $\alpha$ -Toc was evaluated by determining and comparing the adsorption capacity of MIPs for  $\alpha$ -Toc, Trolox, and DBHQ, respectively (Supporting Information Figure S2). The  $Q$  values for  $\alpha$ -Toc, Trolox, and DBHQ are 2.49, 0.025, and 0.454 mg/g, respectively, indicating a good selectivity of the synthesized MIPs toward  $\alpha$ -Toc. The specific differences of the molecular structures of these three compounds give rise to different interaction modes between analyte and polymeric matrices. This factor plays an important role in explaining the significant differences noted for the distinct adsorption capacities between the two structural analogues and  $\alpha$ -Toc.

Most studies that have quantitated the  $\alpha$ -Toc concentration in vegetable oils or biological samples require sample pretreatment, such as saponification, which entails multiple steps of solvent extraction and sample concentration. Inevitably, this procedure results in longer times for sample analyses and subsequently may cause partial degradation because  $\alpha$ -Toc is known to be sensitive to air, alkaline, and light. In the current study, sample pretreatment is not necessary due to the application of MIPs-SPE to separate  $\alpha$ -Toc from other components in vegetable oils. In addition, our MIPs-SPE offered a recovery of  $\sim 80\%$  for  $\alpha$ -Toc in vegetable oils, whereas the recovery of NIPs-SPE was only  $\sim 30\%$ .

Generally, noncovalent imprinting is easier to achieve and applies to a wider variety of templates than covalent imprinting.<sup>37</sup> Held only weakly by noncovalent interactions, such as hydrogen bonding, electrostatic interaction, and coordination bond formation, template molecules are easily removed from polymers under mild conditions. Compared to covalent imprinting, noncovalent imprinting suffers the major disadvantage that the imprinting process is less clear-cut. In other words, the monomer–template adduct is labile and reaction is not strictly stoichiometric.<sup>38</sup>

**Determination of SERS Spectral Features of  $\alpha$ -Toc in Vegetable Oils.** In the current study, we employed silver dendrite as SERS-active substrate for the collection of Raman signals. In the preliminary experiment, we adjusted the reaction time and concentration of silver ions to achieve the best SERS effect using pyridine as a Raman reporting molecule. Both

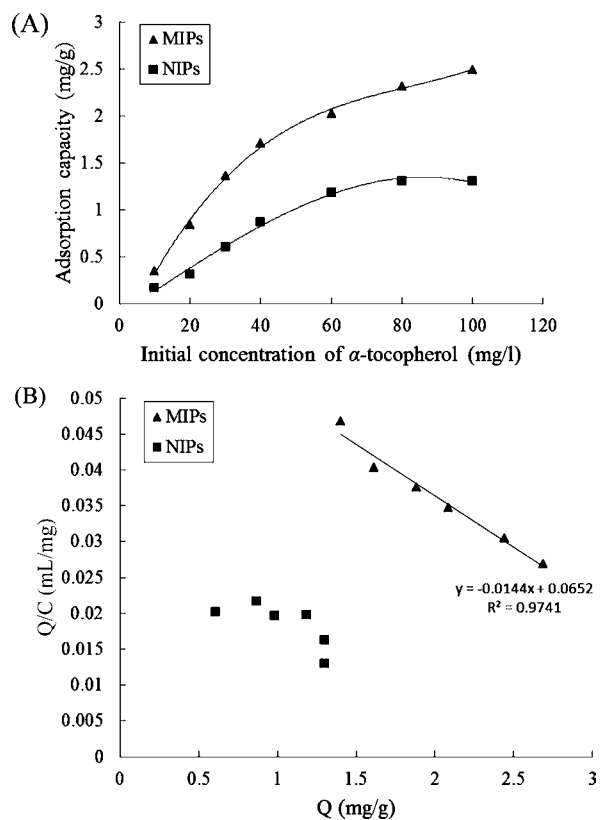


**Figure 2.** (A) Binding isotherm of molecularly imprinted polymers (MIPs) and nonimprinted polymers (NIPs) for  $\alpha$ -tocopherol ( $n = 3$ ); (B) Scatchard plot of MIPs and NIPs toward  $\alpha$ -tocopherol ( $n = 3$ ).

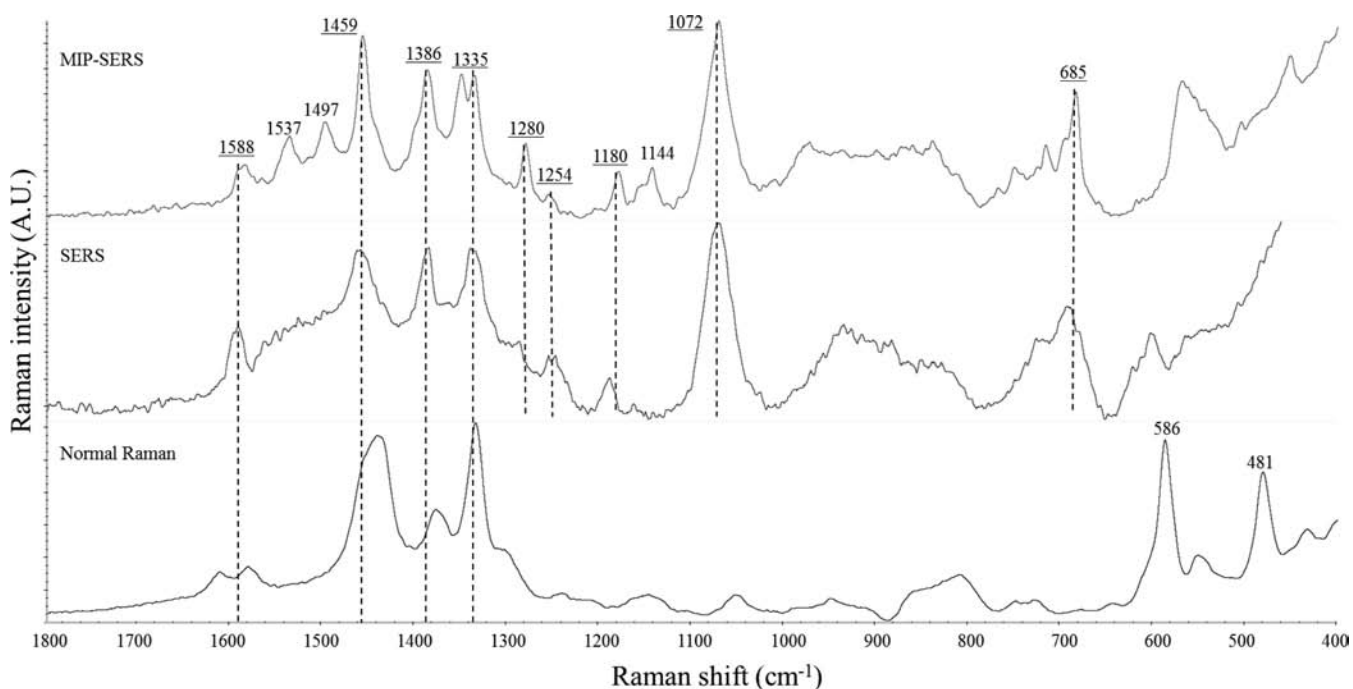


**Figure 3.** Representative spectral features of  $\alpha$ -tocopherol (from bottom to top: normal Raman, SERS, and MIPs-SERS). The underlined numbers denote the specific band from MIPs-SERS, SERS, and/or normal Raman was at the same wavenumber.

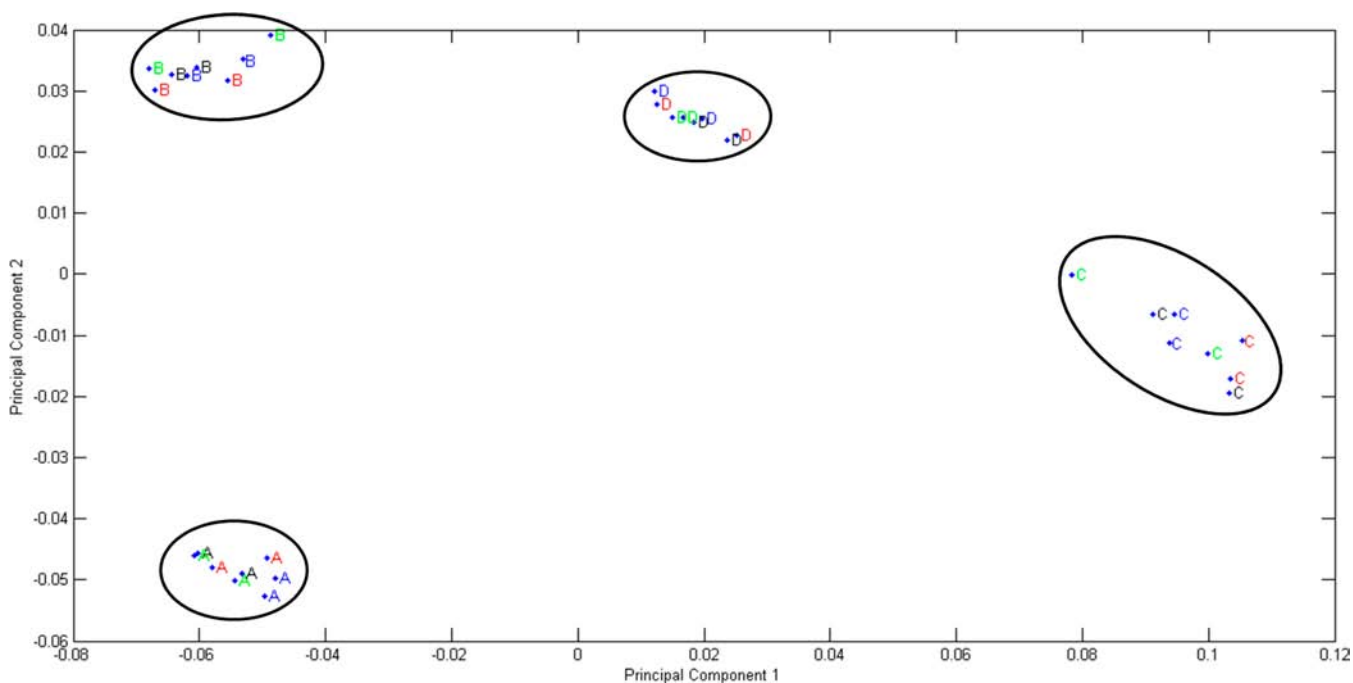


**Figure 4.** Representative two-dimensional principal component analysis for segregation of different concentrations of  $\alpha$ -tocopherol in various categories of vegetable oils. A, B, C, and D represent spiked level of  $\alpha$ -tocopherol at 0, 0.1, 0.5, and 1 mg into 0.05 g vegetable oils, respectively; black, red, green, and blue colors indicate peanut oil, olive oil, corn oil, and canola oil, respectively.

reaction time and concentration affect the size and morphology of the silver dendrite, resulting in various SERS spectral features. Uniform anisotropic growth of silver nanostructure, achieved by using  $\text{AgNO}_3$  solution (200 mmol/L) with a cleaned zinc plate for a total reaction time of 60 s at 22 °C, reliably produced thermally stable silver dendrite structures (Supporting Information Figure S3). Calculating and comparing band intensity and corresponding concentration of the

analyte, we estimate that our developed silver dendrite can enhance the Raman signal by a factor of about  $10^4$ . Other studies have developed silver dendrite nanostructures using galvanic displacement on various metal foils and plates as active SERS substrates. For example, Gutes et al.<sup>27</sup> used aluminum foil and silver fluoride as the substances for generating silver dendrite as a SERS-active substrate for Raman signal enhancement of 1,2-benzenedithiol, 1-phenylethyl mercaptan, and 2,2'-

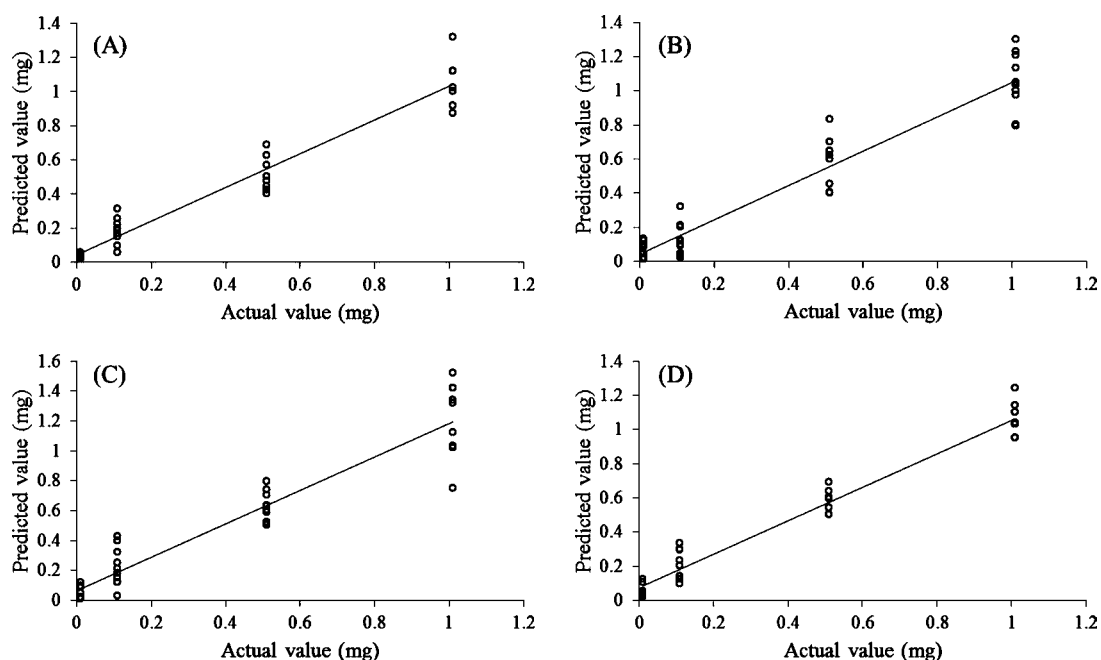


**Figure 5.** Representative partial least-squares regression model for actual spiked  $\alpha$ -tocopherol content into 0.05 g of different types of vegetable oils: (A) peanut oil; (B) olive oil; (C) corn oil; (D) canola oil.

**Table 1.** PLSR Models for Prediction of  $\alpha$ -Tocopherol Content in Vegetable Oils<sup>a</sup> ( $n = 3$ )

SERS spectra	spiked value (mg)	no. of samples	no. of latent variables	R cal	RMSE cal <sup>b</sup>	R val	RMSE val <sup>c</sup>
peanut oil	0, 0.1, 0.5, 1	35	7	$\geq 0.97$	$\leq 0.22$	$\geq 0.94$	$\leq 0.19$
olive oil	0, 0.1, 0.5, 1	38	6	$\geq 0.96$	$\leq 0.41$	$\geq 0.93$	$\leq 0.36$
corn oil	0, 0.1, 0.5, 1	40	6	$\geq 0.95$	$\leq 0.17$	$\geq 0.92$	$\leq 0.13$
canola oil	0, 0.1, 0.5, 1	32	9	$\geq 0.98$	$\leq 0.33$	$\geq 0.96$	$\leq 0.28$

<sup>a</sup>0.05 g of vegetable oil was used for spiking experiment. <sup>b</sup>RMSE cal: root-mean-square error of calibration. <sup>c</sup>RMSE val: root-mean-square error of validation.

dithiodipyridine under illumination at 633 nm. In another study, Wen et al.<sup>28</sup> synthesized silver nanodendrites with the size of 20–30 nm in a stem and branch structure and 5–50  $\mu\text{m}$  in length using a suspension of zinc microparticles as the heterogeneous agent. The application of pyridine as the probing molecule yielded a significant enhancement effect of Raman signal. Recently, Xu et al.<sup>39</sup> reported a cost-effective strategy to synthesize silver dendrite using copper foil under hydrothermal condition in which silver dendrites with different growth directions were prepared by adjusting the content of polyvinylpyrrolidone.

The normal Raman, SERS, and MIPs-SERS spectral features of  $\alpha$ -Toc are shown in Figure 3, and the band assignment is summarized in Table S1 of the Supporting Information. The spectral features reflected the molecular structure of  $\alpha$ -Toc. The bands at wavenumbers of 1335, 1386, 1459, and 1588  $\text{cm}^{-1}$  are assigned to  $\text{CH}_2$ ,  $\text{CH}_3\text{CH}_2$ ,  $\text{CH}_3$ , and  $\text{C}=\text{C}$  vibrational modes, respectively, and these bands appeared at the same wavenumber for normal Raman, SERS, and MIPs-SERS, with a minor shift at 1459  $\text{cm}^{-1}$  in normal Raman. This uniformity emphasizes the reliability of silver dendrite nanostructure as a SERS-active substrate and the efficient separation of MIPs for  $\alpha$ -Toc in vegetable oils. In addition, other prominent bands (i.e., bands at 685, 1180, 1254, and 1280  $\text{cm}^{-1}$ ) are also located at the same wavenumber between SERS and MIPs-SERS, indicating MIPs could effectively retain  $\alpha$ -Toc and remove other interferences from vegetable oils. The bands with minor

intensity at 1144, 1497, and 1537  $\text{cm}^{-1}$  may be derived from oil residues, whereas conventional Raman bands at 586 and 481  $\text{cm}^{-1}$  do not appear in SERS and MIPs-SERS spectra. The band at 1072  $\text{cm}^{-1}$ , used as an internal standard, arises from the  $\text{NO}_3^-$  residues on the silver dendrite substrate. Taken together, the MIPs-SERS biosensing system can be used to effectively separate and detect  $\alpha$ -Toc in vegetable oils and potentially other liquid foods.

The raw MIPs-SERS spectra of samples spiked with different amounts of  $\alpha$ -Toc showed minor variations. Figure S4 of the Supporting Information presents second-derivative transformations of spectra over a range of  $\alpha$ -Toc concentrations in vegetable oils. We attribute the featured band at 1386  $\text{cm}^{-1}$  to a  $\text{CH}_3$  group on the  $\alpha$ -Toc chain. The intensity of this band increased with increasing spiked  $\alpha$ -Toc concentration. The second-derivative transformed MIPs-SERS bands at 1180, 1280, 1459, and 1497  $\text{cm}^{-1}$  showed the same trend, but the band intensities for  $\alpha$ -Toc spiked at levels of 0.5 and 1.0 mg were very similar and could not be differentiated.

An unsupervised two-dimensional PCA model was constructed to segregate the vegetable oil samples spiked with different contents of  $\alpha$ -Toc. This cluster analysis was conducted according to the MIPs-SERS spectral features between the wavenumber regions of 600–1800  $\text{cm}^{-1}$  using Matlab. Each group was well separated and tightly clustered with interclass distance ranging from 15.93 to 34.01 based upon Mahalanobis distance measurements computed between the centroids of

classes (Figure 4). Clusters with interclass distance values  $>3$  are believed to be significantly different from each other.<sup>33</sup> In each cluster, different colors denote different types of vegetable oils (i.e., peanut, olive, corn, and canola oils). This indicates that the MIPs could effectively remove oil components before SERS spectral collection, providing the basis for a reliable biosensing system.

PLSR using the wavenumbers from 600 to 1800  $\text{cm}^{-1}$  defined a linear regression between spiked contents of  $\alpha$ -Toc in vegetable oils and the corresponding MIPs-SERS spectral features (Figure 5). A leave-one-out cross-validation provides a test of model reliability. Table 1 summarizes the major parameters derived from this analysis. A reliable PLSR model should have a high regression coefficient ( $R > 0.90$ ) and a low root-mean-square error (RMSE) of both calibration and cross-validation. Furthermore, the number of latent variables for PLSR model construction should be  $<10$ ; otherwise, model overfitting will occur, resulting in unreliable prediction of other tested samples.<sup>32</sup> The PLSR models that we constructed and validated satisfied these requirements. Therefore, we conclude that this MIPs-SERS biosensing system performs well for both detection and quantification of  $\alpha$ -Toc in vegetable oils.

The current method to detect  $\alpha$ -Toc in foods is HPLC-based analysis. In this study, HPLC-DAD could determine different spiked contents of  $\alpha$ -Toc in vegetable oils. After MIPs-SPE, the detection time is  $\sim 10$  min per sample, including running and column washing. In the food industry, a large amount of samples need to be analyzed in a short time, and HPLC is not ideal for high-throughput detection. On the contrary, SERS can rapidly determine a batch of samples (i.e., 10 s per sample after MIPs-SPE). Furthermore, HPLC-DAD has a detection limit at the parts per million level. Theoretically, the detection limit for SERS can reach the single-molecule level,<sup>8</sup> although this is not the objective in this study because the initial concentration of  $\alpha$ -Toc in different vegetable oils is  $\sim 0.2$  mg/g (using 0.05 g of vegetable oil for MIPs-SPE, the concentration of  $\alpha$ -Toc in the resultant eluting solution is  $\sim 0.8$  ppm). Our preliminary study validated that the detection limit of  $\alpha$ -Toc is  $\sim 10$  ppb using silver dendrite for SERS study. This detection limit does provide SERS as a reliable tool to detect specific chemical compounds (e.g., toxin, antibiotic residue) in foods at the parts per billion level.<sup>7,8</sup>

**Application of MIPs-SERS Biosensor.** The combination of a separation technique with a rapid and highly selective detection technique offers a unique advantage for the quantification of specific analyte in complicated matrices, such as foods. Traditionally, researchers have long relied on multiple extractions by organic solvents to remove major interfering constituents present in food matrices. For example, Zhang et al.<sup>11</sup> applied three different extraction protocols to remove natural interfering components in fish samples before SERS detection of drug residues. The authors observed that residues of these components adversely affected the quantification of Raman spectral features of drug residues. Generally speaking, one cannot rely on organic solvent extraction to remove all of the substances interfering with the detection of a given analyte. Moreover, even if a tedious solvent-based sample pretreatment improves the quality of the SERS signal, these steps tremendously increase the analysis time.

The application of first/second-derivative transformations and segregation-based multivariate analysis models (e.g., principal component analysis of cluster model and hierarchical cluster analysis of dendrogram model) can magnify minor

spectral variation to improve spectral differentiation to some degree. However, challenges exist to gaining specificity for real applications. For example, a food sample may contain multiple antibiotic residues, and this can make it difficult to resolve spectral patterns. Moreover, the presence of structural analogues can interfere with analysis owing to the overlap of similar SERS spectral patterns.

Other studies have applied a selective separation followed by SERS for the detection of trace levels of biochemical hazards in foods. For example, one recent study used antibody-based immunomagnetic separation or aptamer separation to separate and enrich foreign protein in milks and subsequently applied SERS for detection.<sup>15,16</sup> It is worth noting that here, with the antibody component or aptamer conjugated to the surface of noble metal nanosubstrate, an enhanced signal contribution from the antibody or aptamer could not be avoided, complicating spectral interpretation. Furthermore, although antibodies are natural, they will become unstable outside their native environment. In some cases the needed receptor may be in short supply.<sup>20</sup>

Our MIPs model offers a highly efficient alternative method to achieve selective separation of analytes from a great number of interfering compounds. In essence, we imprint a molecular memory on the polymer, enabling the polymer to selectively rebind the template. MIPs differ from biological receptors because they are rigid, large, and insoluble, whereas their natural counterparts are flexible, small, and soluble in most cases.<sup>20</sup> After loading, washing, and eluting, analytes isolated in solution can be directly deposited onto silver dendrite nanostructures for SERS signal collection.

In conclusion, we have developed a rapid and accurate MIPs-SERS biosensing system for the determination of  $\alpha$ -Toc in vegetable oils. This biosensing system demonstrates good sensitivity and selectivity for the detection of specific analyte molecules in a complicated matrix. Future work will focus on conjugating MIPs within SERS substrates to realize a “one-step” biosensing system to detect various chemical constituents and contamination in agricultural and food products.

## ■ ASSOCIATED CONTENT

### 📄 Supporting Information

Additional table and figures. This material is available free of charge via the Internet at <http://pubs.acs.org>.

## ■ AUTHOR INFORMATION

### Corresponding Authors

\*(S.W.) E-mail: [s.wang@tust.edu.cn](mailto:s.wang@tust.edu.cn)

\*(X.L.) E-mail: [xiaonan.lu@ubc.ca](mailto:xiaonan.lu@ubc.ca)

### Funding

This work was supported by funds awarded to X.L. by the University of British Columbia new faculty start-up grant and a British Columbia vitamin research fund (10R09963) as well as by funds awarded to S.W. by the Ministry of Science and Technology of China (2011CB512014 and 2012CB720803).

### Notes

The authors declare no competing financial interest.

## ■ ACKNOWLEDGMENTS

We thank Huey Kuan and Yazheng Liu for technical assistance.

## ■ REFERENCES

- (1) Lemaire-Ewing, S.; Desrumaux, C.; Néel, D.; Lagrost, L. Vitamin E transport, membrane incorporation and cell metabolism: is  $\alpha$ -tocopherol in lipid rafts an oar in the lifeboat? *Mol. Nutr. Food Res.* **2010**, *54*, 631–640.
- (2) Bauernfeind, J.; Desai, I. The tocopherol content of food and influencing factors. *Crit. Rev. Food Sci. Nutr.* **1977**, *8*, 337–382.
- (3) Atkinson, J.; Harroun, T.; Wassall, S. R.; Stillwell, W.; Katsaras, J. The location and behavior of  $\alpha$ -tocopherol in membranes. *Mol. Nutr. Food Res.* **2010**, *54*, 641–651.
- (4) Sature, M. T.; Huang, S.-W.; Frankel, E. N. Effect of natural antioxidants in virgin olive oil on oxidative stability of refined, bleached, and deodorized olive oil. *J. Am. Oil Chem. Soc.* **1995**, *72*, 1131–1137.
- (5) Rock, C. L.; Jacob, R. A.; Bowen, P. E. Update on the biological characteristics of the antioxidant micronutrients: vitamin C, vitamin E, and the carotenoids. *J. Am. Diet. Assoc.* **1996**, *96*, 693–702.
- (6) Kopec, R. E.; Schweiggert, R. M.; Riedl, K. M.; Carle, R.; Schwartz, S. J. Comparison of high-performance liquid chromatography/tandem mass spectrometry and high-performance liquid chromatography/photo-diode array detection for the quantitation of carotenoids, retinyl esters,  $\alpha$ -tocopherol and phyloquinone in chylomicron-rich fractions of human plasma. *Rapid Commun. Mass Spectrom.* **2013**, *27*, 1393–1402.
- (7) Lu, X.; Al-Qadiri, H. M.; Lin, M.; Rasco, B. A. Application of mid-infrared and Raman spectroscopy to the study of bacteria. *Food Bioprocess Technol.* **2011**, *4*, 919–935.
- (8) Ellis, D. I.; Brewster, V. L.; Dunn, W. B.; Allwood, J. W.; Golovanov, A. P.; Goodacre, R. Fingerprinting food: current technologies for the detection of food adulteration and contamination. *Chem. Soc. Rev.* **2012**, *41*, 5706–5727.
- (9) Lu, X.; Samuelson, D. R.; Xu, Y.; Zhang, H.; Wang, S.; Rasco, B. A.; Xu, J.; Konkel, M. E. Detecting and tracking nosocomial methicillin-resistant *Staphylococcus aureus* using a microfluidic SERS biosensor. *Anal. Chem.* **2013**, *85*, 2320–2327.
- (10) Haynes, C. L.; McFarland, A. D.; Duyn, R. P. V. Surface-enhanced Raman spectroscopy. *Anal. Chem.* **2005**, *77*, 338A–346A.
- (11) Zhang, Y.; Lai, K.; Zhou, J.; Wang, X.; Rasco, B. A.; Huang, Y. A novel approach to determine leucomalachite green and malachite green in fish fillets with surface-enhanced Raman spectroscopy (SERS) and multivariate analyses. *J. Raman Spectrosc.* **2012**, *43*, 1208–1213.
- (12) Zhang, Y.; Huang, Y.; Zhai, F.; Du, R.; Liu, Y.; Lai, K. Analyses of enrofloxacin, furazolidone and malachite green in fish products with surface-enhanced Raman spectroscopy. *Food Chem.* **2012**, *135*, 845–850.
- (13) Lin, M.; He, L.; Awika, J.; Yang, L.; Ledoux, D.; Li, H.; Mustapha, A. Detection of melamine in gluten, chicken feed, and processed foods using surface enhanced Raman spectroscopy and HPLC. *J. Food Sci.* **2008**, *73*, T129–T134.
- (14) Di Anibal, C. V.; Marsal, L. F.; Callao, M. P.; Ruisánchez, I. Surface enhanced Raman spectroscopy (SERS) and multivariate analysis as a screening tool for detecting Sudan I dye in culinary spices. *Spectrochim. Acta Part A: Mol. Biomol. Spectrosc.* **2012**, *87*, 135–141.
- (15) He, L.; Haynes, C. L.; Diez-Gonzalez, F.; Labuza, T. P. Rapid detection of a foreign protein in milk using IMS–SERS. *J. Raman Spectrosc.* **2011**, *42*, 1428–1434.
- (16) Lamont, E. A.; He, L.; Warriner, K.; Labuza, T. P.; Sreevatsan, S. A single DNA aptamer functions as a biosensor for ricin. *Analyst* **2011**, *136*, 3884–3895.
- (17) Temur, E.; Zengin, A.; Boyaci, I. S. H.; Dudak, F. C.; Torul, H.; Tamer, U. U. Attomole sensitivity of *Staphylococcal* enterotoxin B detection using an aptamer-modified surface-enhanced raman scattering probe. *Anal. Chem.* **2012**, *84*, 10600–10606.
- (18) He, L.; Deen, B. D.; Pagel, A. H.; Diez-Gonzalez, F.; Labuza, T. P. Concentration, detection and discrimination of *Bacillus anthracis* spores in orange juice using aptamer based surface enhanced Raman spectroscopy. *Analyst* **2013**, *138*, 1657–1659.
- (19) Ramström, O.; Skudar, K.; Haines, J.; Patel, P.; Brüggemann, O. Food analyses using molecularly imprinted polymers. *J. Agric. Food Chem.* **2001**, *49*, 2105–2114.
- (20) Haupt, K. Peer reviewed: molecularly imprinted polymers: the next generation. *Anal. Chem.* **2003**, *75*, 376A–383A.
- (21) Puoci, F.; Cirillo, G.; Curcio, M.; Iemma, F.; Spizzirri, U.; Picci, N. Molecularly imprinted solid phase extraction for the selective HPLC determination of  $\alpha$ -tocopherol in bay leaves. *Anal. Chim. Acta* **2007**, *593*, 164–170.
- (22) Liu, H.; Fang, G.; Zhu, H.; Li, C.; Liu, C.; Wang, S. A novel ionic liquid stabilized molecularly imprinted optosensing material based on quantum dots and graphene oxide for specific recognition of vitamin E. *Biosens. Bioelectron.* **2013**, *47*, 127–132.
- (23) Liu, H.; Fang, G.; Li, C.; Pan, M.; Liu, C.; Fan, C.; Wang, S. Molecularly imprinted polymers on ionic liquid-modified CdSe/ZnS quantum dots for the highly selective and sensitive optosensing of tocopherol. *J. Mater. Chem.* **2012**, *22*, 19882–19887.
- (24) Qian, K.; Fang, G.; He, J.; Pan, M.; Wang, S. Preparation and application of a molecularly imprinted polymers for the determination of trace metolcarb in food matrices by high performance liquid chromatography. *J. Sep. Sci.* **2010**, *33*, 2079–2085.
- (25) Gimeno, E.; Castellote, A.; Lamuela-Raventós, R.; De la Torre, M.; López-Sabater, M. Rapid determination of vitamin E in vegetable oils by reversed-phase high-performance liquid chromatography. *J. Chromatogr., A* **2000**, *881*, 251–254.
- (26) Bonvehí, J. S.; Coll, F. V.; Rius, I. A. Liquid chromatographic determination of tocopherols and tocotrienols in vegetable oils, formulated preparations, and biscuits. *J. AOAC Int.* **2000**, *83*, 627–634.
- (27) Gutiérrez, A.; Carraro, C.; Maboudian, R. Silver dendrites from galvanic displacement on commercial aluminum foil as an effective SERS substrate. *J. Am. Chem. Soc.* **2010**, *132*, 1476–1477.
- (28) Wen, X.; Xie, Y.-T.; Mak, W. C.; Cheung, K. Y.; Li, X.-Y.; Renneberg, R.; Yang, S. Dendritic nanostructures of silver: facile synthesis, structural characterizations, and sensing applications. *Langmuir* **2006**, *22*, 4836–4842.
- (29) Fang, J.; You, H.; Kong, P.; Yi, Y.; Song, X.; Ding, B. Dendritic silver nanostructure growth and evolution in replacement reaction. *Cryst. Growth Des.* **2007**, *7*, 864–867.
- (30) He, L.; Lin, M.; Li, H.; Kim, N. J. Surface-enhanced Raman spectroscopy coupled with dendritic silver nanosubstrate for detection of restricted antibiotics. *J. Raman Spectrosc.* **2010**, *41*, 739–744.
- (31) Lu, X.; Liu, Q.; Benavides-Montano, J. A.; Nicola, A. V.; Aston, D. E.; Rasco, B. A.; Aguilar, H. C. Detection of receptor-induced glycoprotein conformational changes on enveloped virions by using confocal micro-Raman spectroscopy. *J. Virol.* **2013**, *87*, 3130–3142.
- (32) Lu, X.; Huang, Q.; Miller, W. G.; Aston, D. E.; Xu, J.; Xue, F.; Zhang, H.; Rasco, B. A.; Wang, S.; Konkel, M. E. Comprehensive detection and discrimination of *Campylobacter* species by use of confocal micro-Raman spectroscopy and multilocus sequence typing. *J. Clin. Microbiol.* **2012**, *50*, 2932–2946.
- (33) Lu, X.; Rasco, B. A.; Kang, D. H.; Jabal, J. M.; Aston, D. E.; Konkel, M. E. Infrared and Raman spectroscopic studies of the antimicrobial effects of garlic concentrates and diallyl constituents on foodborne pathogens. *Anal. Chem.* **2011**, *83*, 4137–4146.
- (34) Wang, S.; Liu, L.; Fang, G.; Zhang, C.; He, J. Molecularly imprinted polymers for the determination of trace ractopamine in pork using SPE followed by HPLC with fluorescence detection. *J. Sep. Sci.* **2009**, *32*, 1333–1339.
- (35) Pan, M.; Wang, J.; Fang, G.; Tang, W.; Wang, S. Synthesis and characterization of a molecularly imprinted polymers and its application as SPE enrichment sorbent for determination of trace methimazole in pig samples using HPLC-UV. *J. Chromatogr., B* **2010**, *878*, 1531–1536.
- (36) Duan, Z.; Yi, J.; Fang, G.; Fan, L.; Wang, S. A sensitive and selective imprinted solid phase extraction coupled to HPLC for simultaneous detection of trace quinoxaline-2-carboxylic acid and methyl-3-quinoxaline-2-carboxylic acid in animal muscles. *Food Chem.* **2013**, *139*, 274–280.



(37) Haupt, K. molecularly imprinted polymers in analytical chemistry. *Analyst* **2001**, *126*, 747–756.

(38) Bui, B. T. S.; Haupt, K. molecularly imprinted polymers: synthetic receptors in bioanalysis. *Anal. Bioanal. Chem.* **2010**, *398*, 2481–2492.

(39) Xu, H.; Shao, M.; Chen, T.; Zhao, Y.; Lee, S. T. Surface-enhanced Raman scattering on silver dendrite with different growth directions. *J. Raman Spectrosc.* **2012**, *43*, 396–404.